

# Fabrication of Hydrophobic Structures by Nanosecond Pulse Laser

Yukui Cai<sup>a</sup>, Ana M. L. Sousa<sup>b</sup>, King Hang Aaron Lau<sup>b</sup>, Wenlong Chang<sup>a</sup> and Xichun Luo<sup>a,1</sup>

<sup>a</sup>*Centre for Precision Manufacturing, DMEM, University of Strathclyde, UK*

<sup>b</sup>*WestCHEM/Department of Pure & Applied Chemistry, University of Strathclyde, UK*

**Abstract.** In this paper, a feasibility study of manufacturing anti-bacteria surface on stainless steel 7C27Mo2 used for surgical tools by using nanosecond pulse laser is presented. The effect of laser power on the depth of groove was studied through laser cutting experiment. Micro-pillar arrays of different dimensions and spacing were generated by laser cutting. The wetting characteristics of micro-structured surfaces were assessed by using the static contact angle measurement approach. The measurement results show that the original hydrophilic stainless steel surface can be converted into a hydrophobic surface by using laser structuring as the contact angle can be doubled. This research shows that it is feasible to manufacture hydrophobic microstructures with a laser cutting process.

**Keywords.** Hydrophobicity, laser cutting, contact angle

## 1. Introduction

Nature has made many natural functional surfaces for different creatures. For example, the lotus leaves exhibit the unusual wetting characteristics of superhydrophobicity and self-cleaning property [1]. In addition, Gecko feet comprise of spinules, its length varying from several hundred nanometres to several microns. Such micro and nano structures on its skin provide a superhydrophobic and an antibacterial action where Gram-negative bacteria (*Porphyromonas gingivalis*) are killed when exposed to the surface [2]. According to the detailed surface structures of natural lotus leaf or Gecko's feet, we have mimicked the superhydrophobic surfaces on various substrates. These functional surfaces have many practical applications, such as self-cleaning, corrosion protection and anti-icing, drag reduction and anti-bacteria.

In medical applications, bacterial adhesion on surgical tool or implants is a critical factor resulting in device-associated infection. Tang investigated the contact angle effect on bacterial adhesion behaviour [3]. The experimental results show that the superhydrophobic surface shows high resistance to bacterial contamination. With the increase of contact angle, the number of bacteria decreased, especially *Staphylococcus aureus* in vitro [3]. Therefore, manufacturing hydrophobic surface can be the first step in

---

<sup>1</sup> Xichun Luo, Centre for Precision Manufacturing, DMEM, University of Strathclyde, UK; E-mail: xichun.luo@strath.ac.uk.

achieving antimicrobial function. Hydrophobicity is commonly evaluated by the contact angle of a deionized water droplet over a surface.

There are various approaches for the preparation of hydrophobic surfaces such as electro-chemical deposition [4], plasma etching method [5], sol-gel processing [6, 7], chemical etching [8], micro cutting [9], laser cutting [10, 11] and so on., Laser cutting approach is a contactless and especially effective machining approach to manufacturing micro structures on variety of materials. Vorobyev created a multifunctional surface on platinum, titanium, and brass metal, such as light absorption, superhydrophobicity, and self-cleaning property, by producing a hierarchical micro-nanostructure with femtosecond laser pulses [11]. Groenendijk's study shows that the most critical dimensions for hydrophobic structures are the height of the pillars and the distance between them. Moreover, a superhydrophobic polypropylene surface with contact angles of  $165^\circ$  and a very small hysteresis was achieved by femto second laser pulses [10]. However, manufacturing of hydrophobic structures on medical stainless steel 7C27Mo2, which is widely used on medical instrument, has not been explored to any notable extent.

In this work, a fiber laser with 100 ns pulse duration was used to fabricate micro structures on 7C27Mo2. First of all, the laser cutting experiment for optimization of laser processing parameters is performed. Then, micro structures of different sizes are manufactured on the samples. Finally, the Wenzel model and Cassie-Baxter model are used to predict the static contact angle and compared with the measured value.

## 2. Laser cutting experiments

### 2.1 Experimental set-up

The laser cutting experiments have been carried out on a hybrid ultra-precision machine shown in Figure 1. Its milling spindle has a maximum rotational speed of 125,000 rpm. And it is also equipped with a 20W nanosecond laser with pulse duration of 100 ns, a central emission wavelength of 1064 nm and a maximum pulse repetition rate of 200 kHz. The laser beam passes through a lens and focuses onto the sample surface, which is mounted on a precision X-Y-Z stage. The workpiece with a dimension of  $10\text{ mm} \times 10\text{ mm} \times 1\text{ mm}$  is made of 7C27Mo2 stainless steel.

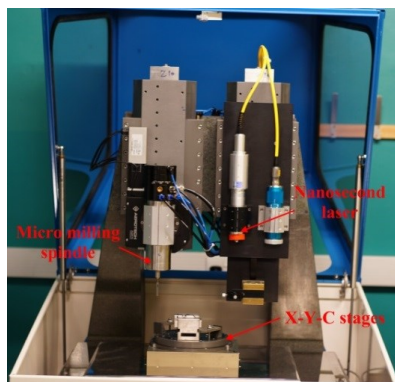


Figure 1. Hybrid ultraprecision machine.

## 2.2 Laser cutting parameter optimization

The laser cutting experiment parameters are listed in Table 1. The grooves as the preliminary test patterns and machined at different laser powers is shown in Figure 2.

**Table 1.** The laser cutting parameters in the experiments

Laser power percentage	Pulse repetition rate	Feed rate
10%-90% (2 W-18 W)	100K	100mm/min

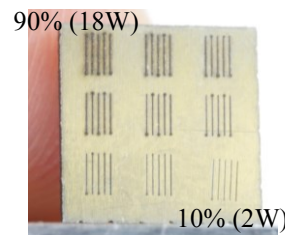
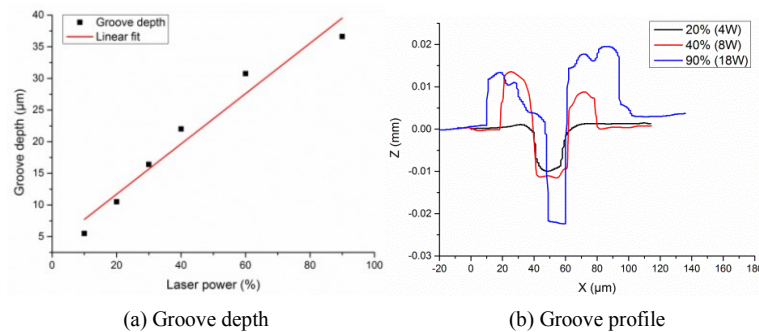


**Figure 2.** Picture of grooves machining at different laser power.

Alicona G4 optical profiling system was used to measure the depth of micro groove and shown in Figure 3. With the increase of laser power, the groove depth varied from 5.5  $\mu\text{m}$  to 36.6  $\mu\text{m}$ . As shown in Figure 3 (b), with the increase of laser power, the heat effect area was clearly observed, molten materials stacked on both sides of the groove. Thus, the groove quality surface was getting worse.



(a) Groove depth

(b) Groove profile

**Figure 3.** Groove depth and profile vary with laser power.

## 3. Fabrication of micro structures and prediction of its hydrophobicity

Seven samples with micro pillars of different spacing varying from 10  $\mu\text{m}$  to 80  $\mu\text{m}$  were designed. According to the result of processing parameter optimization, these samples were processed at a laser power of 20% (4W), other parameters being the same as in Table 1. Unidirectional machining was employed to generate micro grooves on the sample surface by the horizontal laser cutting strategy. After slotting the whole surface of the samples, vertical cutting with the same step distance was employed to obtain the final micro pillar structures.

Two typical models have been developed to describe the behavior of a droplet on rough surfaces (as shown in Figure 4 (a) and (b)), which are the Wenzel [12, 13] and Cassie-Baxter models [14,15]. According to the Wenzel model, the droplet maintains

contact with the structures and penetrates the asperities, and the surface contact area is increased as shown in Figure 4 (a). In addition, the static contact angle  $\theta_w$  can be predicted by Eq. (1). Alternatively, according to the Cassie-Baxter model, the droplet is not able to wet the microstructure spaces and its static contact angle  $\theta_{CB}$  can be predicted by Eq. (2).

$$\cos \theta_w = r \cos \theta \quad (1)$$

$$\cos \theta_{CB} = -1 + f(1 + \cos \theta) \quad (2)$$

$$r = \frac{\text{actual surface area}}{\text{planar area}} = 1 + \frac{4ah}{(a+b)^2} \quad (3)$$

$$f = \frac{\text{actual contact area}}{\text{planar area}} = \frac{a^2}{(a+b)^2} \quad (4)$$

where,  $r$  is the roughness factor which can be calculated by Eq. (3) for micro pillars.  $f$  is the fraction of asperities and can be calculated by Eq. (4).  $a$  is the width of the pillar,  $b$  is the width of the groove,  $h$  is the height of the pillar as shown in Figure 5. where,  $b=20 \mu\text{m}$ ,  $h=10 \mu\text{m}$ .

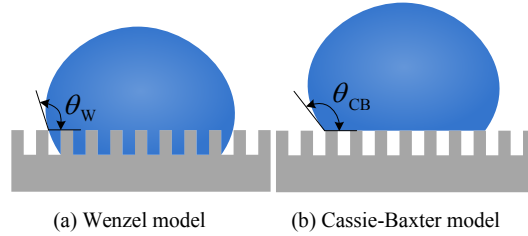


**Figure 4.** Wetting behaviour of water droplet.

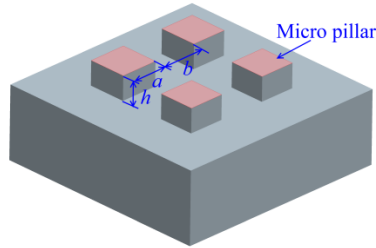


**Figure 5.** Geometry model of micro pillars.

According to Eqs. (1)-(4), the static contact angle under different states can be calculated. At the same time, actual contact angles can be measured by the sessile drop method. First of all, a needle extrudes a water droplet on the sample. Then, the contact angle can be measured with the aid of an industrial camera and image processing software on a PC (a Krüss DSA25B Drop Shape Analyser was used for all measurements).

The side view of water droplets on the smooth surface before machining, captured by the contact angle goniometer camera, is shown in Figure 6. The average contact angle  $\theta$  was  $50.0^\circ$ . The water droplets on the smooth surface exhibited a contact angle lower than  $90^\circ$ . Therefore, 7C27Mo2 can be considered a hydrophilic material, which is easy for bacterial adhesion and biofilm generation.

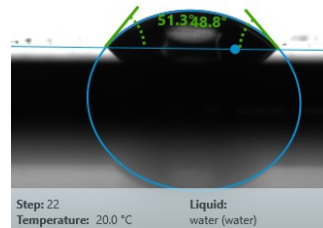


**Figure 6.** Water droplet on the smooth surface.

The comparison between theoretical and experimental values of contact angle is shown in Figure 7. The contact angle of samples with  $a=10\ \mu\text{m}$  and  $20\ \mu\text{m}$  is higher than the value predicted by the Wenzel model, but lower than the Cassie-Baxter model prediction. Hence, the water droplet belongs to the case of partial wetting, between the Wenzel and Cassie-Baxter states (i.e. the heterogeneous state). However, with the increase of pillar width ( $a$ ), the contact angle is very close to the value predicted by Cassie-Baxter model. Thus, from  $30\ \mu\text{m}$  to  $80\ \mu\text{m}$ , the water droplet is suspended on the micropillars, matching the Cassie-Baxter state.

For  $a=20\ \mu\text{m}$ ,  $30\ \mu\text{m}$  and  $40\ \mu\text{m}$ , the contact angle of samples is about  $110^\circ$ , which is twice of contact angle of the smooth surface. With the further increase of pillar width, the contact angle shows a declining trend due to the increasing fraction of asperities  $f$ . According to Eq. (2), there is an inversely proportional relationship between  $\theta_{CB}$  and  $f$ .

All of these results show that laser microstructuring is an effective method for increasing the surface hydrophobicity. It can turn 7C27Mo2 from a hydrophilic material into more hydrophobic one.

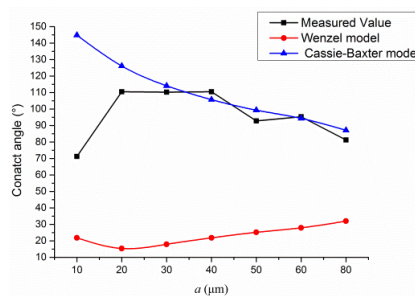


**Figure7.** Comparison of theoretical and experimental values of contact angle.

#### 4. Conclusions

In this paper, the effect of laser power on the depth of groove in laser structuring stainless steel 7C27Mo2 was studied. The experimental results show that the depth of groove increased from  $5.5\ \mu\text{m}$  to  $36.6\ \mu\text{m}$  with the increase of laser power 4 W to 18 W. The

wetting characteristics of hydrophobic micro-pillars machined by laser structuring process have been investigated. It shows that the original hydrophilic surface can be converted into a more hydrophobic surface. The contact angle can be doubled to 110°. Therefore this research shows that it is feasible to manufacture hydrophobic microstructures with a laser structuring process.

## 5. Acknowledgements

This research was undertaken in the context of MICROMAN project (“Process Fingerprint for Zero-defect Net-shape MICROMANufacturing”, <http://www.microman.mek.dtu.dk/>). MICROMAN is a European Training Network supported by Horizon 2020, the EU Framework Programme for Research and Innovation (Project ID: 674801). The authors would also gratefully acknowledge the financial support from the EPSRC (EP/K018345/1) for this research. We thank the Stewart fund in the chemistry department which partially funded the purchase of the contact angle instrument.

## References

- [1] Sun T, et al., Bioinspired surfaces with special wettability, *Accounts of chemical research* 38 (2005), 644-652.
- [2] Watson, Gregory S., et al., A gecko skin micro/nano structure—A low adhesion, superhydrophobic, anti-wetting, self-cleaning, biocompatible, antibacterial surface, *Acta biomaterialia*, 21 (2015), 109-122.
- [3] Tang, Peifu, et al., Effect of superhydrophobic surface of titanium on staphylococcus aureus adhesion, *Journal of Nanomaterials* 2011 (2011), 2.
- [4] Shirtcliffe, Neil J., et al., Dual-scale roughness produces unusually water-repellent surfaces, *Advanced Materials*, 16(2004), 1929-1932.
- [5] Kinoshita, Hiroshi, et al., Superhydrophobic/superhydrophilic micropatterning on a carbon nanotube film using a laser plasma-type hyperthermal atom beam facility, *Carbon*, 48 (2010), 4403-4408.
- [6] Latthe, Sanjay S., et al., Superhydrophobic silica films by sol-gel co-precursor method, *Applied Surface Science*, 256 (2009), 217-222.
- [7] Ganbavle, Vinayak V., et al., Self-cleaning silica coatings on glass by single step sol-gel route, *Surface and Coatings Technology*, 205 (2011), 5338-5344.
- [8] Xiu, Yonghao, et al., Hierarchical silicon etched structures for controlled hydrophobicity/superhydrophobicity, *Nano letters*, 7 (2007), 3388-3393.
- [9] Zhenyu, Shi, et al., Prediction of contact angle for hydrophobic surface fabricated with micro-machining based on minimum Gibbs free energy, *Applied Surface Science*, 364 (2016), 597-603.
- [10] Groenendijk, Max., Fabrication of super hydrophobic surfaces by fs laser pulses, *Laser Technik Journal*, 5 (2008), 44-47.
- [11] Vorobyev, A. Y., and ChunleiGuo. "Multifunctional surfaces produced by femtosecond laser pulses." *Journal of Applied Physics* 117.3 (2015): 033103
- [12] Wenzel, Robert N, Resistance of solid surfaces to wetting by water, *Industrial & Engineering Chemistry*, 28 (1936), 988-994.
- [13] Wenzel, Robert N, Surface roughness and contact angle, *The Journal of Physical Chemistry*, 53 (1949), 1466-1467.
- [14] Cassie, A. B. D., and S. Baxter, Wettability of porous surfaces, *Transactions of the Faraday society*, 40 (1944), 546-551.
- [15] Cassie, A. B. D., Contact angles, *Discussions of the Faraday Society*, 3 (1948), 11-16.